

PREDICTION OF CRACK INITIATION IN LAMINATES WITH FIBER DISCONTINUITY: A VARIATIONAL APPROACH

M. J. Mohammad Fikry¹, Vladimir Vinogradov² and Shinji Ogihara³

¹ Department of Mechanical and Aerospace Engineering, Tokyo University of Science, 2641 Yamazaki, Noda-shi, Chiba-ken, 278-8510, Japan, fikry@rs.tus.ac.jp

² School of Engineering, Newcastle University,

Newcastle upon Tyne, NE1 7RU, UK, vladimir.vinogradov@newcastle.ac.uk

³ Department of Mechanical and Aerospace Engineering, Tokyo University of Science, 2641 Yamazaki, Noda-shi, Chiba-ken, 278-8510, Japan, ogihara@rs.tus.ac.jp

Keywords: Variational mechanics, Energy criterion, Composite laminates, Damage prediction, Resin pocket

ABSTRACT

Composite laminates with continuous fibre are strong and stiff but due to the presence of fibre discontinuity, the stress concentration may cause damage to occur and lower its mechanical properties. Therefore, it is necessary to evaluate the influence of fibre discontinuity on the mechanical properties of the laminates and its damage behaviour. This work extends the applicability of the variational approach method for analysing laminates with alternating materials in the longitudinal directions based on the original variational model of Hashin's analysis. The stress analysis considered an arbitrary number of regions with different material properties and herein we specifically used the analysis to evaluate laminates with fibre/ply discontinuity. For simplicity, we assumed a plane stress condition or stress distribution, we assumed that the normal stress in the loading direction was constant along the direction of thickness in each ply. The admissible stress state that satisfied both equilibrium and boundary/continuity conditions was constructed with unknown functions that were determined using the principle of minimum complementary energy. The finite fracture criterion was then used to describe the onset of matrix crack in the resin pocket. The critical energy release rate was calculated and used to predict the crack onset stress in the laminate with different numbers of discontinuous ply and length of the resin pocket. These results were compared with experimental results, which obtained good agreement.

1 INTRODUCTION

In the practical industry setting, to obtain a cost-effective optimum design, prepregs are sometimes cut at some locations which result in the existence of a fibre discontinuous part in the laminates. Composite laminates with continuous fibre are strong and stiff but due to the presence of fibre discontinuity, the stress concentration may cause damage to occur and lower its mechanical properties [1-4]. Therefore, it is necessary to evaluate the influence of fibre discontinuity on the mechanical properties of the laminates and its damage behaviour. A variational analysis approach has been used in this study to determine the stress state in a laminate with ply discontinuity, subject to loading. This work extends the applicability of the variational approach method for analysing laminates with alternating materials in the longitudinal directions based on the original variational model of Hashin's analysis [5]. The extended version of this analysis applies for arbitrary N-regions problem where in this specific study of the laminate with ply discontinuity, the location of the crack can be arbitrary in the resin-rich region. Fig. 1 shows an illustration of a laminate with a resin-rich region associated with fibre discontinuity where it is noted that the analysis for this laminate structure needs to be formulated in the context of a laminate with three divided subregions in the longitudinal direction. This stress analysis then was used to calculate the energy release rate due to the formation of a crack that occurred in the resin-rich region. This critical energy release rate then was used to predict the crack onset stress in the laminate with different numbers of discontinuous ply and length of the resin pocket.

2 EXPERIMENT

Unidirectional (UD) $[0]_8$ laminates with two, four and six discontinuous plies in the middle, with a resin pocket length less than 0.1 mm were manufactured and tension-tested using a TENSILON RTF-1350 tensile testing machine. In addition, laminates with four discontinuous plies, with different resin pocket length were also manufactured. The specimens and their (resulting) post-cured gap lengths, L_0 are listed in Table 1. Using an autoclave, the prepregs were then cured at a temperature of 130 °C and pressure of 0.2 MPa; the laminate's post-cured thickness was 1.18 mm (averaged). The laminates were then cut into specimens as shown in Fig. 1. A monotonic tensile loading was then applied at a crosshead speed of 0.5 mm/min. To observe the deformation and damage occurring on the edges of the specimens, an in-situ optical microscope, KEYENCE VHX-1000 (lens: MX-7575CS) was used.

Table 1 Specimens and post-cured resin's gap length in UD laminate.

Specimens		Post-cured resin's gap length, L_0
Small gap (<0.1 mm)	1	28.4 μm
	2	30.9 μm
	3	65.6 μm
About 1 mm gap	4	1.24 mm
	5	1.34 mm
	6	1.38 mm
About 2 mm gap	7	1.73 mm
About 3 mm gap	8	3.41 mm

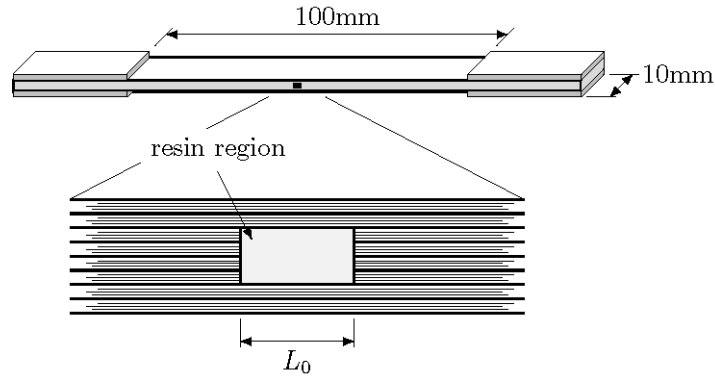


Figure 1: Schematic of specimen measurement.

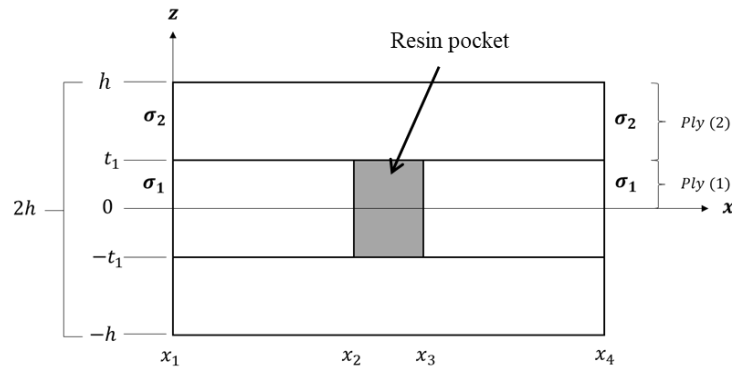


Figure 2: Analysis model.

3 ANALYSIS METHOD

The simplified geometry adopted for this analysis consists of a rectangular resin region of thickness t_1 , length L_0 and unit depth. An illustration of a laminate with a resin region is shown in Fig. 2. The

interfaces between the resin pocket and the discontinuous ply, as well as the cracks in the resin are assumed to be flat and normal to the laminate and loading direction x . This assumption is expected to be accurate for cracks having small curvature. An admissible stress field for a laminate with a resin pocket and with or without cracks is constructed that satisfies equilibrium, traction continuity conditions at the interfaces, zero traction on the external surfaces and open crack surfaces, and minimizes the complementary energy functional.

3.1 Construction of admissible stress field

As an example to demonstrate this analysis, an illustration of a unidirectional laminate with a resin-rich region associated with ply discontinuity is shown in Fig. 2. In this analysis, the number of regions (or the segments of materials) along the longitudinal direction can be arbitrary. Here, a two-ply system is considered, while a symmetry condition about the x -axis ($z=0$) is applied. We first assume that the longitudinal normal stress σ_{xx} in each ply (m) varies only along the x -direction:

$$\sigma_{xx}^{(m)} = \phi_m(x), \quad (1)$$

where m is the ply number and $\phi_1(x)$ and $\phi_2(x)$ are unknown functions to be determined. For the stress defined in Eq. (1) to be admissible for its use in the principle of minimum total complementary energy, stresses $\sigma_{xz}^{(m)}$, $\sigma_{zz}^{(m)}$, along with $\sigma_{xx}^{(m)}$ have to satisfy all equilibrium equations and traction continuity conditions. The resulting stresses of other stress components are

$$\sigma_{xx}^{(1)} = \phi(x), \quad (2)$$

$$\sigma_{xx}^{(2)} = \frac{N_{xx}}{t_2} - \left(\frac{t_1}{t_2}\right)\phi(x), \quad (3)$$

$$\sigma_{xz}^{(1)} = -\phi'(x)z, \quad (4)$$

$$\sigma_{xz}^{(2)} = \left(\frac{t_1}{t_2}\right)\phi'(x)(z-h), \quad (5)$$

$$\sigma_{zz}^{(1)} = \frac{1}{2}\phi''(x)(z^2 - ht_1), \quad (6)$$

$$\sigma_{zz}^{(2)} = -\frac{1}{2}\left(\frac{t_1}{t_2}\right)\phi''(x)(h-z)^2. \quad (7)$$

3.2 Variational formulation

The complementary energy U_c associated with the admissible stresses in a laminate subject to traction boundary conditions is defined by

$$U_c = \frac{1}{2}S_{ijkl}^*\sigma_{ij}^0\sigma_{kl}^0V, \quad (8)$$

where S_{ijkl}^* are the effective compliances of the composite and $V = hL$ is the volume of the model of unit depth. In general, for region (i) bounded by $x_i \leq x \leq x_{i+1}$, the complementary energy is given by

$$U_{ca}^{(i)} = \int_{x_i}^{x_{i+1}} \left[\int_0^{t_1} W_1^{(i)} dz + \int_{t_1}^h W_2^{(i)} dz \right] dx, \quad (9)$$

$W_m^{(i)}$ is the energy density for ply m ($m = 1,2$) in region (i). Substitution of expressions in Eq. (2)-(7) for the resulting stresses into the energy density $W_m^{(i)}$ and integration over the laminate thickness in z -direction in Eq. (9) yields the complementary energy for each region:

$$U_{ca}^{(i)} = \frac{1}{2} \int_{x_i}^{x_{i+1}} \left[\psi_i - C_0^{(i)} \phi^{(i)} + C_{00}^{(i)} \phi^{(i)2} + C_2^{(i)} \phi^{(i)''} + C_{02}^{(i)} \phi^{(i)} \phi^{(i)''} + C_{22}^{(i)} \phi^{(i)''2} + C_{11}^{(i)} \phi^{(i)'}{}^2 \right] dx, \quad (10)$$

where primes denote derivatives with respect to x . In conjunction with the principle of minimum complementary energy, Euler-Lagrange equation was used thus gives the solution of the system as

$$\phi^{(i)}(x) = A_1^{(i)} e^{\eta_1^{(i)} x} + A_2^{(i)} e^{\eta_2^{(i)} x} + A_3^{(i)} e^{\eta_3^{(i)} x} + A_4^{(i)} e^{\eta_4^{(i)} x} + B^{(i)}, \quad (11)$$

where A_1, A_2, A_3 , and A_4 are the constants to be determined from the boundary conditions and $B^{(i)}$ is the far-field stress in ply 1 of region i . Summing up the complementary energy for the whole unit cell, we have the total complementary energy,

$$U_{ca}^{total} = \sum_{i=1}^N 2U_{ca}^{(i)}, \quad (12)$$

Here, N is the total number of regions.

3.3 Determining the region boundary stresses that minimize the complementary energy

By some mathematical means of integration by parts and rearranging it according to the order of derivatives, we can write the total complementary energy in Eq. (10) in the terms of regions' boundary stresses as

$$U_{ca}^{total} = \{f\}^T [Q] \{f\} + \{q\}^T \{f\} + \sum_{i=1}^N Q_0^{(i)}, \quad (13)$$

where $\{f\} = \{\phi_1, \phi_1', \phi_2, \phi_2', \dots, \phi_{N+1}, \phi_{N+1}'\}^T$ is a $2(N+1) \times 1$ vector for region boundary stresses, and the coefficients are placed in $2(N+1) \times 2(N+1)$ matrix $[Q]$ and $2(N+1) \times 1$ vector $\{q\}$. Here, ϕ_i and $\phi^{(i)'}$ is the normal stress and shear stress component respectively at $x = x_i$ ($\phi_i = \phi^{(i)}(x_i)$, $\phi_i' = \phi^{(i)'}(x_i)$). Taking the readily known boundary conditions (at both edges of the laminate) as the dependent variables in $\{f\}$, and extracting only the unknown stresses (at the inner boundaries) as the independent variables, $\{\hat{f}\}$, they can easily be determined by subsequent minimization of $U_{ca}^{(total)}$ using partial differentiation:

$$\frac{\partial U_{ca}^{total}}{\partial \{\hat{f}\}} = [\hat{Q} + \hat{Q}^T] \{\hat{f}\} + \{\hat{q}\} = 0, \quad (14)$$

where now, $\{\hat{f}\} = \{\phi_2, \phi_2', \phi_3, \phi_3', \dots, \phi_N, \phi_N'\}^T$, while $[\hat{Q}]$ and $\{\hat{q}\}$ are the matrix/vector of coefficients associated with the unknown stresses. Solving the simultaneous equations resulting from Eq. (14) gives the values of boundary stresses,

$$\{\hat{f}\} = [\hat{Q} + \hat{Q}^T]^{-1} \cdot \{\hat{q}\}. \quad (15)$$

Solution of Eq. (15) determines constants A (Eq. (11)), which provide the final expressions for the stress functions $\phi^{(i)}$ (Eq. (11)) and consequently defines the entire admissible stress field that gives the minimum complementary energy. However, it is to be noted that the dependency on the interval lengths in Eq. (13) disappears only in case the intervals near to the tips are long enough, so the interfaces do not interact.

3.4 Calculation of critical energy release rate (ERR) and prediction of crack onset stress

In this study, we used the finite fracture criterion to describe the onset of matrix crack in the resin pocket. The criterion has been employed by several authors, e.g. Refs. [6-8], assuming instantaneous formation of a finite crack area and describing progressive cracking as a series of discrete fracture

events. For a laminate developing a through-the-ply crack at x , the critical energy release rate (ERR) is calculated as

$$G_C = \frac{\Delta U_{ca}(x)}{\Delta A_c}, \quad (16)$$

where ΔU_{ca} is the change in the complementary energy due to a crack occurrence at x and ΔA_c is the crack area. In the present case, the ERR associated with the crack formation is defined by the difference between the energies of a cracked laminate with one crack and the uncracked laminate:

$$G_C = \frac{(U'_{ca} - U_{ca})\sigma_c^2}{A_c\sigma_0^2}. \quad (17)$$

Here, U'_{ca} and U_{ca} is the complementary energy of cracked and uncracked laminates respectively, σ_c is the crack onset stress from experiment result and σ_0 is the applied axial stress. In this study, we used the crack onset stress $\sigma_c=196$ MPa from a laminate with four discontinuous plies and resin pocket length of $65.6\mu\text{m}$, which gives $G_C= \text{J/m}^2$. The crack onset stresses for laminates with different number of discontinuous plies and resin pocket length were then calculated using

$$\sigma_c = \sqrt{\frac{A\sigma_0^2 G_C}{U'_{ca} - U_{ca}}}. \quad (18)$$

4 RESULTS AND DISCUSSION

4.1 Experimental results

Fig. 3 shows the edge's optical observation of crack appearance with an increasing tensile load and the corresponding average applied stress in a laminate specimen with the resin gap length, $L_0 = 0.0656$ mm. This specimen was taken to represent the results of laminate with a very short resin gap (<0.1 mm) as a similar damage behavior can be observed in all specimens. Based on the observation in this figure, a single crack appeared at the edge of the specimen in the resin pocket at the applied stress of 195 MPa. However, it is unclear whether the crack that occurred here is located precisely at the interfaces between the resin and the discontinuous UD ply or in the middle of the resin as the resin gap is too short and the resin pocket's geometry (fiber cut lining) is uneven. We yet can assume that the crack occurred at the interfaces by observing the edge corner of the resin pocket, as it followed the shape of the interfaces (see Fig 3, applied stress of 433 MPa).

The edge's optical observation of specimen with the length of the resin region, $L_0 = 1.73$ mm is shown in Fig. 4. For specimens with a larger resin pocket length (larger than 1 mm), although the exact crack locations with respect to the interfaces and the stresses vary slightly from one specimen to another, the presented cracking pattern is representative for all tested specimens of similar geometry and length of the resin pocket. From the images, it can be observed that the crack forms not at the interface but at a distance from the interfaces between the resin and the discontinuous UD ply (at 470 MPa).

Fig. 5 and 6 shows the microscopic edge observation and the X-ray images showing the damage initiation and growth at different stress levels for 2 and 6-ply discontinuity specimen, respectively. Comparing the results in these two figures and Fig. 3, it can be observed that the number of discontinuous plies significantly affects the crack onset stress; crack occurred early in laminates with larger number of discontinuous plies.

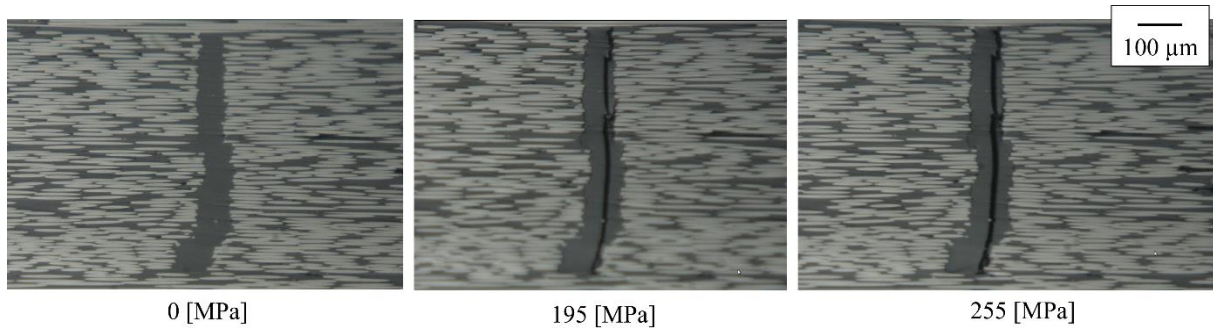


Figure 3: Edge microscopic images of laminate with four discontinuous plies, with 0.0656 mm resin gap at different stress levels.

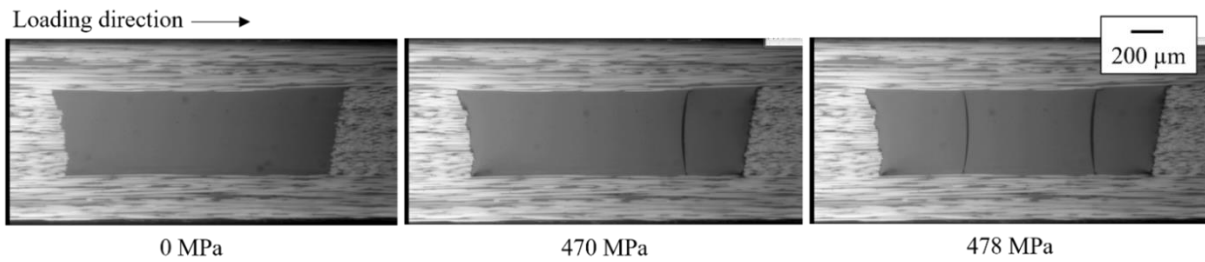


Figure 4: Edge microscopic images of laminate with four discontinuous plies, with 1.73 mm resin gap at different stress levels.

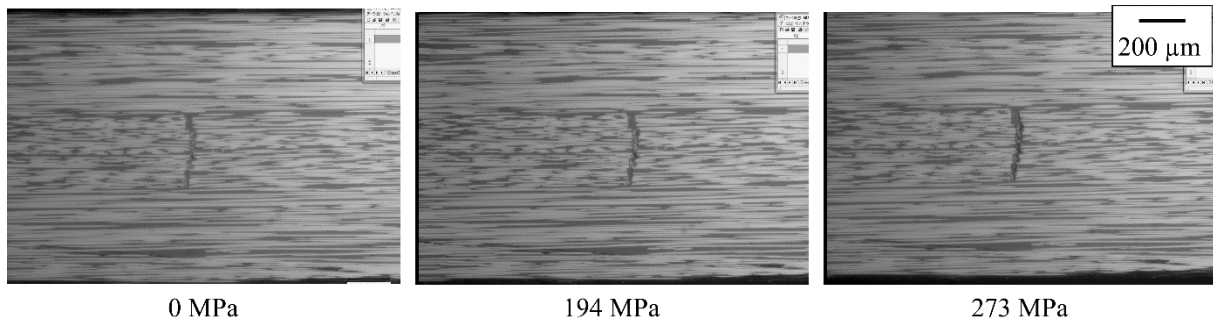


Figure 5: Edge microscopic images of laminate with two discontinuous plies at different stress levels.

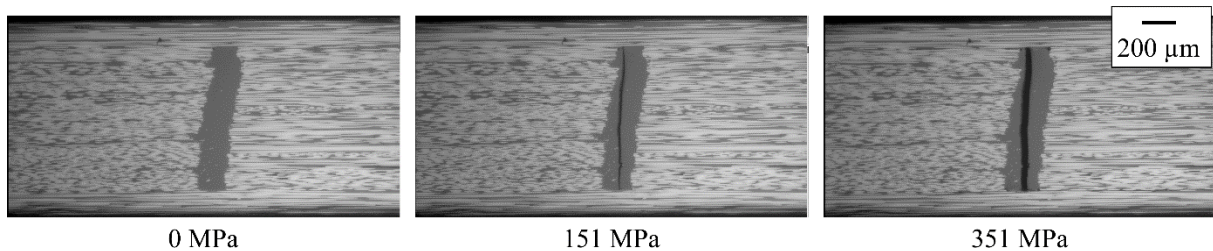


Figure 6: Edge microscopic images of laminate with six discontinuous plies at different stress levels.

4.2 Analytical results

Here, the material properties of CFRP ply measured in [9] were used. The properties of the epoxy resin were assumed as $E = 3 \text{ GPa}$, $\nu = 0.3$. Figs. 7 and 8 show the ERR as a function of x -distance of crack from the centre of the resin pocket for a laminate (with four discontinuous plies) with 0.0656 mm and 1.73 mm resin pocket length, respectively. These two laminates were presented here as the representative of a laminate with a long ($>0.1 \text{ mm}$) resin pocket length and a laminate with a resin a very short ($<0.1 \text{ mm}$) resin pocket length. The value of the calculated maximum ERR associated with the crack location determines the critical ERR, which for the specimen with a very short resin pocket, was estimated $G_c \approx 461.2 \text{ J/m}^2$ while for the specimen with a long resin pocket was estimated $G_c \approx 570.3$

J/m^2 . For the laminate with a very short resin pocket, the ERR reaches its maximum at the middle of the resin pocket (Fig. 7), but the value itself is not significantly vary compared to other x-distance. In experiment, it is also difficult to define the location of the crack as the resin pocket is too short (Fig. 3). On the other hand, for the laminate with a long resin pocket, the ERR reaches its maximum at the interface of CFRP ply and resin pocket (Fig. 8), hence, cannot explain the observed cracking pattern in Fig. 4. This might happen due to the chemical shrinkage of the resin that introduces some residual stresses in the resin pocket, as was explained in [2].

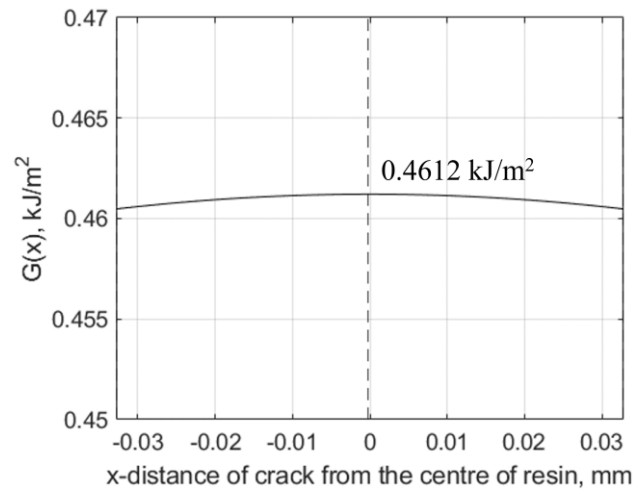


Figure 7: Energy release rate as a function of x-distance of crack from the centre of the resin pocket for a laminate with four discontinuous plies, with a 0.0656 mm resin pocket length.

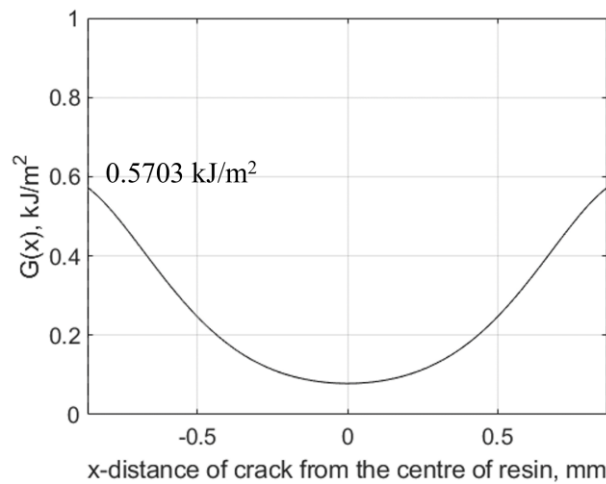


Figure 8: Energy release rate as a function of x-distance of crack from the centre of the resin pocket for a laminate with four discontinuous plies, with a 1.73 mm resin pocket length.

Based on the results in Figs. 7 and 8, we distinguished the assumption of crack's location for the prediction of crack onset stresses for laminates with different resin pocket length; crack occurred at the centre of the resin pocket in laminates with a resin pocket length less than 0.1 mm, while crack occurred at the interface in laminates with a resin pocket length more than 0.1 mm. Fig. 9 shows the prediction of crack onset stress for laminates with different resin pocket length (with comparison to experimental result), assuming that the crack occurred at (a) the centre of the specimen ($G_c=461.2 \text{ J/m}^2$), and at (b) the interface between CFRP ply and resin pocket ($G_c=570.3 \text{ J/m}^2$). Fig. 10 on the other hand shows the enlarged view of Fig. 8 for the resin pocket length less than 0.1 mm. It can be seen that the analytical results are in good agreement with the experimental results.

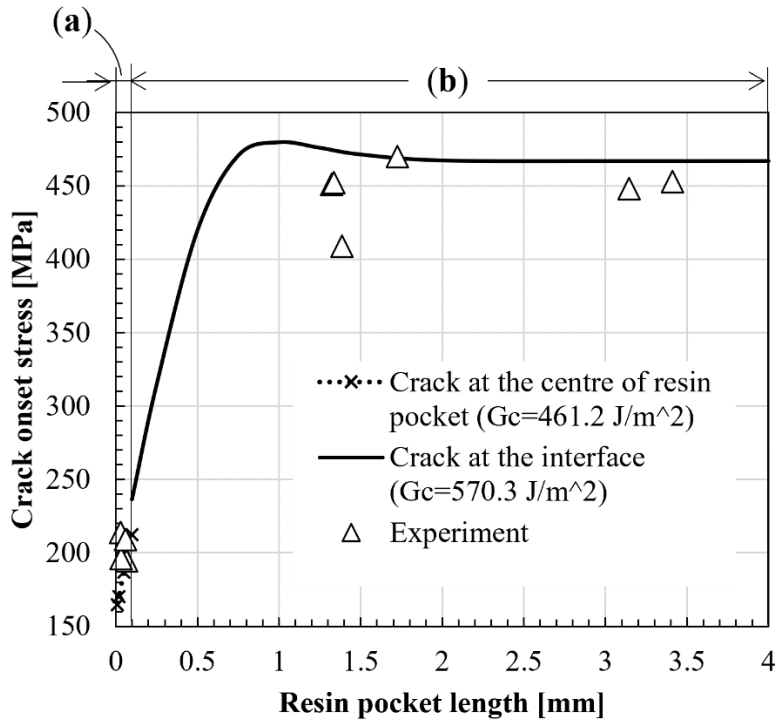


Figure 9: Prediction of crack onset stress for laminates with different resin pocket length (with comparison to experimental result), assuming that the crack occurred at (a) the centre of the specimen ($G_c=461.2$ J/m²), and at (b) the interface between CFRP ply and resin pocket ($G_c=570.3$ J/m²).

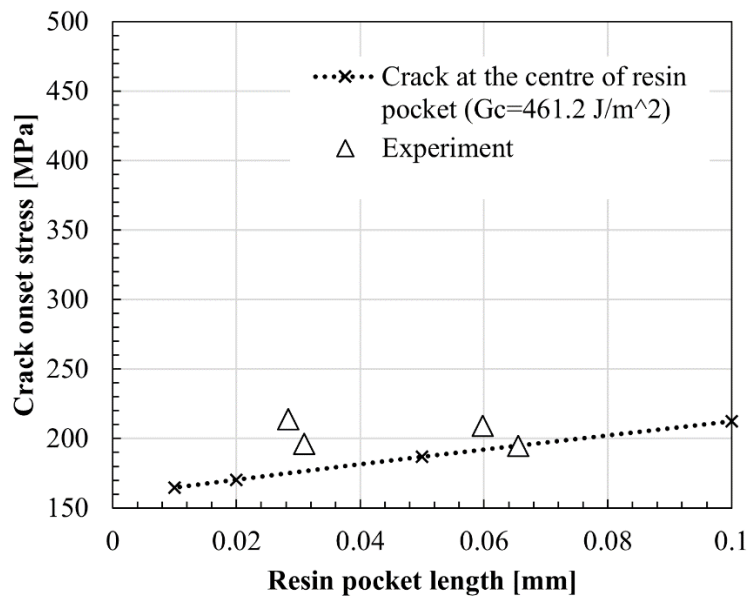


Figure 10: Enlarged view of prediction of crack onset stress for laminates with different resin pocket length in Figure 8 for laminates with <0.1 mm resin pocket length.

For the prediction of crack onset stresses in laminates with different number of discontinuous plies, we used a laminate with a very short resin pocket (<0.1 mm) for the comparison with the available experimental results. In this case, the critical ERR used was 461.2 J/m², taken from the highest ERR obtained in Fig. 7 for a laminate with a resin pocket length of 0.0656 mm (Fig. 3). Fig. 2 and Fig. 3 shows the result for prediction of the crack onset stress in laminates with different number of discontinuous plies and resin-rich region gap length respectively. As shown in the figure, the predicted crack onset stresses for laminates with two and six discontinuous plies are in an excellent agreement

with the experimental results.

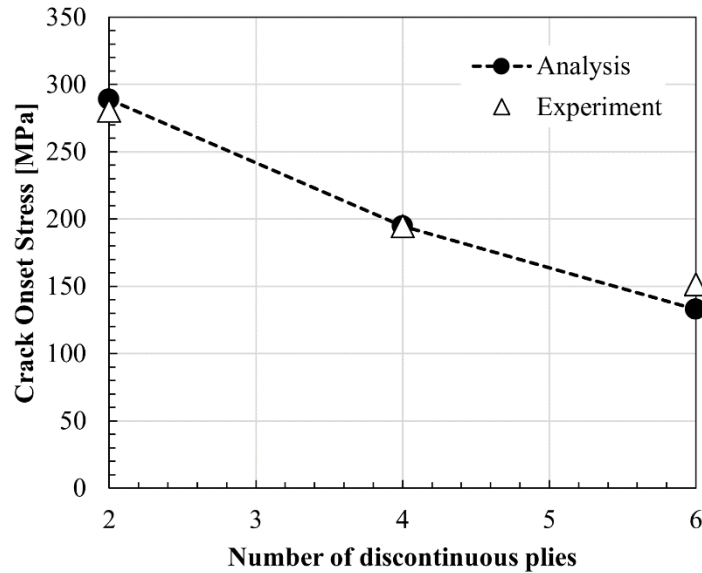


Figure 11: Prediction of crack onset stress for laminates with different number of discontinuous plies (with comparison to experimental result).

This study showed that the developed analysis using the minimum complementary energy based on the variational model of Hashin's analysis [5] can be used to calculate the energy release rate thus can predict the crack onset stresses in laminates with ply discontinuity. However, it should be noted that the analysis introduced here used a plane stress approach for simplicity purposes, therefore only some simple material configurations such as UD and cross-ply laminates could be analyzed. To increase the applicability of the analysis, the stress components in width direction of the laminate should be taken account. Besides, thermal effects were not considered here, which should be done to increase the accuracy of the cracking prediction. Also, natural boundary conditions such as been used in [10] and/or ply refinement technique [11] should be considered in the future to overcome the limitation of two-ply system problem and to increase the accuracy of the analysis.

5 CONCLUSION

A variational model for analysis of stress fields in laminates with regions of different material properties along the longitudinal direction (such as ply discontinuity) subjected to uniaxial loading was developed based on the original variational model of Hashin's analysis. The analysis was then used to predict the matrix cracking formation in CFRP laminates with ply discontinuity. The critical energy release rate was calculated and used to predict the crack onset stress in the laminate with different numbers of discontinuous ply and length of the resin pocket. The results were then compared with experimental results, which obtained good agreement.

ACKNOWLEDGEMENTS

This work was partly supported by a research grant from Hirose Foundation.

REFERENCES

- [1] M. Fikry, Q. Wang, M. Irita, S. Ri, N. Toyama, V. Vinogradov and S. Ogihara, Measurement of microscopic strain distributions of CFRP laminates with fiber discontinuities by sampling moiré method, *Advanced Composite Materials*, **31**, 3, 2022, pp. 273-288 (doi: [10.1080/09243046.2021.1975208](https://doi.org/10.1080/09243046.2021.1975208)).

- [2] M. Fikry, V. Vinogradov and S. Ogihara, Experimental observation and modeling of resin pocket cracking in unidirectional laminates with ply discontinuity, *Composites Science and Technology*, **218**, 2022, p. 109175 (doi: [10.1016/j.compscitech.2021.109175](https://doi.org/10.1016/j.compscitech.2021.109175)).
- [3] M. Fikry, V. Vinogradov and S. Ogihara, Analytical prediction of the local Young's modulus in CFRP laminate with ply discontinuity: a variational approach, *Advanced Composite Materials*, 2023 (doi: [10.1080/09243046.2023.2165873](https://doi.org/10.1080/09243046.2023.2165873)).
- [4] M. Fikry, V. Vinogradov and S. Ogihara, Mechanical properties and damage behavior of tapered unidirectional CFRP laminates, *Mechanical Engineering Journal*, (2023) (doi: [10.1299/mej.23-00079](https://doi.org/10.1299/mej.23-00079)).
- [5] Z. Hashin, Analysis of cracked laminates: a variational approach, *Mechanics of Materials*, **4**, 2, 1985, pp. 121-136 (doi: [10.1016/0167-6636\(85\)90011-0](https://doi.org/10.1016/0167-6636(85)90011-0)).
- [6] J. Nairn, *Comprehensive Composite Materials*, 2.12 Matrix microcracking in composites, Vol. 2 Oxford, , Pergamon, 2000, pp. 403-432 (doi: [10.1016/B0-08-042993-9/00069-3](https://doi.org/10.1016/B0-08-042993-9/00069-3)).
- [7] Z. Hashin, Finite thermoelastic fracture criterion with application to laminate cracking analysis, *Journal of the Mechanics and Physics of Solids*, **44**, 7, 1996, pp. 1129-1145 (doi: [10.1016/0022-5096\(95\)00080-1](https://doi.org/10.1016/0022-5096(95)00080-1)).
- [8] V. Vinogradov, Z. Hashin, Probabilistic energy based model for prediction of transverse cracking in cross-ply laminates, *International Journal of Solids and Structures*, **42**, 2, 2005, pp. 365-392 (doi: [10.1016/j.ijsolstr.2004.06.043](https://doi.org/10.1016/j.ijsolstr.2004.06.043)).
- [9] M. Fikry, S. Ogihara and V. Vinogradov, The effect of matrix cracking on mechanical properties in FRP laminates, *Mechanics of Advanced Materials and Modern Processes*, **4**, 3, 2018, pp. 1-16 (doi: [10.1186/s40759-018-0036-6](https://doi.org/10.1186/s40759-018-0036-6)).
- [10] M. Hajikazemi, M. Sadr, H. Hosseini-Toudeshky, et al., Thermo-elastic constants of cracked symmetric laminates: a refined variational approach, *International Journal of Mechanical Sciences*, **89**, 2014, pp.47–57 (doi: [10.1016/j.ijmecsci.2014.08.008](https://doi.org/10.1016/j.ijmecsci.2014.08.008)).
- [11] V. Vinogradov, A variational method for analysis of laminates with parallel arrays of intralaminar cracks, *International Journal for Numerical Methods in Engineering.*, **120**, 5, 2019, pp. 666-705, (doi: [10.1002/nme.6152](https://doi.org/10.1002/nme.6152)).